Romanian Reports in Physics **74**, 801 (2022)

OBTAINING THE NATIONAL METROLOGICAL TRACEABILITY CHAIN ASSOCIATED WITH THE DOSIMETRY OF THE EYE LENS BY CREATING HIGH-PRECISION DOSIMETRY PHANTOMS, USING STATE-OF-THE-ART 3D PRINTING TECHNIQUES

M.-R. IOAN, M. ZADEHRAFI*, C. OLARU, G. ORMENISAN, S. CIOBANU, L. TUGULAN

Horia Hulubei National Institute for Physics and Nuclear Engineering,
30 Reactorului, P.O. Box MG-6, RO-077125 Bucharest-Magurele, Romania
* Corresponding author's: *mastaneh.zadehrafi@nipne.ro*

Received March 15, 2022

Abstract. In this work, an innovative method has been proposed to obtain the Romanian national metrological traceability chain associated with eye lens dosimetry. This metrological method is based on using modern 3D printing techniques to create a high-precision human head replica and supporting the experimental results by the Monte Carlo simulations.

Key words: eye lens dosimetry, 3D printing technique, Monte Carlo.

1. INTRODUCTION

As is known [1, 2], the human eye can be exposed to ionizing radiation in many ways such as medical procedures (both patients and medical staff), industry, applied nuclear physics research, etc. One of the most radiation-sensitive parts of the human eye is the eye lens, which could gradually show degradation (*e.g.*, radio-induced cataract) by exposure to ionizing radiation [3, 4]. To provide support for monitoring the absorbed dose by the eye lens, the International Organization for Standardization has issued ISO 15382:2015 "Radiological protection – Procedures for monitoring the dose to the lens of the eye, the skin, and the extremities" [5]. However, its practical implementation is still a challenge, mostly due to the limitation of the actual dose-measuring devices and lack of the calibration protocols [6]. To this end, knowing the precise magnitude of the absorbed dose by the eye lens is of great importance. Furthermore, the applied dosimeters have to be appropriately calibrated and traceable to the national and international dosimetry standards. At a national level in Romania, "Horia Hulubei National Institute for R&D in Physics and Nuclear Engineering (IFIN-HH)" is in charge of performing all the ionizing radiation-related metrology activities. Given the fact that the available dosimeters are not exactly positioned at the eye lens, and also the measured value must be correlated to both eyes, reliable calibration factors are required [5, 7]. There have been earlier studies at the international level in the framework of the ORAMED project (Optimization

of RAdiation protection of MEDical staff), supported by the European Atomic Energy Community [8–11].

For assuring the national metrological traceability chain related to the dosimetry of the eye lens, an innovative metrological method based on using modern 3D printing techniques [12–19] to create high-precision human head dosimetry has been proposed in this work. In the first phase, a human head phantom has been created by a 3D printer, with special attention to the 3D eyeball, having similar geometry and composition as the real eye. Five standard dosimeters (OSL) were attached to the forehead, both eyes, and both temples of the head phantom. Then, it was exposed to a standard ionizing radiation field (Co-60 radionuclide, certified source). After each exposure, the absorbed dose by each of the five dosimeters was determined and registered. Then, the same experimental setup was modeled by the Monte Carlo technique (MCNP6.2 [20–22]) and all the experiments were simulated. The experimental and computational results (the absorbed dose value by each dosimeter) were compared, considering all the involved parameters. The second phase of this study is related to the determination of the uniformity of the ionizing radiation field, in which a special pair of glasses with passive detectors was worn by the head phantom. After gradually reading the dose values along to the radiosensitive parts of the glasses, the uniformity of the radiation field was determined. The final step of the experiment is providing traceable, reliable, and precise calibration factors (with the associated uncertainties) for standard dosimeters placed on the temples, which are considered as commercial dosimeters.

The experimental and simulation parts of this study are explained in Section 2. In Section 3, the obtained results are presented, compared, and discussed in detail. Finally, a summary of the present work along with the concluding remarks is provided in Section 4.

2. MATERIALS AND METHODS

2.1. EXPERIMENTAL MEASUREMENTS

The first stage of this project was to create a human head phantom with a special focus on the eyeball and eye lens. To achieve this objective, a professional 3D printer type Form2 (Formlabs, USA) [23] was applied, which consists of a high-precision laser (250 mW power) guided by custom galvanometers (very high print resolution) and a heated resin tank that creates a reliable printing process for large, solid, and complex details (Fig. 1). Performing a study on the anatomy of the human head (shape, density, and particularities) was required to obtain the essential information regarding the physical effects that occur at the interaction of gamma radiation with it (absorption, attenuation, inelastic scattering, backscattering, *etc.*). Then, a 3D model of the human head skeleton was selected, which was subsequently processed for 3D printing. The 3D object has been decomposed into 5 components so that each of them fits into the maximum print size offered by the printer used

(15×15 mm^2). The material chosen for the phantom is a "Dental SG" photopolymer resin produced by Formlabs laboratories (applicability in the dental field), which is a biocompatible material, with a density equivalent to the bone, designed for a printing resolution of 100 μm.

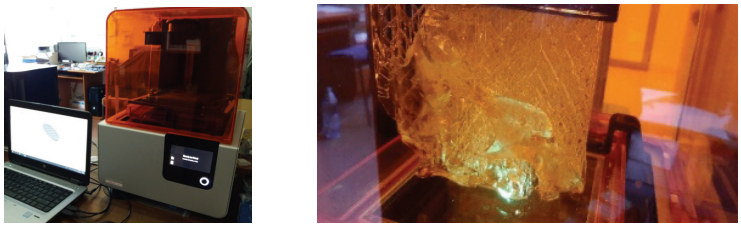

(a) (b)

Fig. 1 – a) The 3D printer Form2 with its accessories;
b) the 3D printer during the printing procedure.

The same procedure has been followed for the human eyeball plus eye lens. A 3D model of the human eye was selected and subsequently processed to be 3D printed separately from the head replica. A type of transparent resin named "Clear Resin" produced by Formlabs laboratories was applied to print the 3D human eye. Figure 2 (a) and (b) show the 3D printed head phantom and the human eye, respectively.

(a) (b)

Fig. 2 – a) The 3D-printed human head; b) the 3D-printed human eye.

After having all the components (skeleton, eyeballs, and eye lenses) printed separately, the final head phantom was assembled and ready to run the experiments. Five standard dosimeters (OSL) were mounted in front of the forehead, both eyes, and both temples of the head phantom (Fig. 3). It is worth mentioning that the two dosimeters mounted on two temples are considered as the commercial dosimeters to be calibrated. In other words, the calibration factors for them could be obtained with respect to the real dose values taken by the eye lenses (discussed in the next section).

The next step was to measure the dose rate of the radioactive Co-60 source. It is a solid source in an Al capsule, fixed in steel support with a rod, which is classified by the National Institute of Metrology as a working standard. It is located in a lead

collimator, placed on the exposure stand in the Ionizing Radiation Metrology Laboratory (LMRI), Department of Radioisotopes and Radiation Metrology (DRMR) within "Horia Hulubei National Institute for R&D in Physics and Nuclear Engineering (IFIN-HH)". To measure the flow rate for the equivalent dose from the Co-60 radioactive source, the dosimeter was placed on the stand support at a distance of 150 cm from the source. The flow rate for the dose equivalent measured at 150 cm from the source was (104.3 ± 4.2) μSv/h on 21.05.2021. This value has ensured traceability to the primary standards of PTB Germany.

Fig. 3 – The 3D human head phantom equipped with five OSL standard dosimeters.

The fully equipped phantom (phantom head with eyes attached in orbits, high precision OSLs attached in front of the forehead, both eyes, and both temples (Fig. 3)) was exposed, using the aforementioned Co-60 source, at 3 equivalent doses: 200 μSv, 400 μSv, and 600 μSv (by different exposure durations). The center of the gamma ionizing radiation field from the Co-60 source was directed perpendicular to the OSL-type detector positioned on the phantom's forehead.

Another set of experiments was performed to have the dosimeter responses for a field of ionizing radiation from a Co-60 source perpendicular to one of the temples. This time, the fully equipped phantom was exposed under the same exposure condition as the above-mentioned experiments at an equivalent dose of 400 μSv, but with the center of the beam directed towards the center of the right temple. This means that the head phantom was rotated 90° to its previous position. In both sets that will be called set 1 and set 2, respectively, the absorbed dose value by each detector was registered and determined by an OSL reader system to be compared with the reference and computational values.

To determine the uniformity of the ionizing radiation field from a radioactive source by RIA (Radiation-Induced Absorption) method, a pair of special glasses was worn by the human head phantom and the equipped phantom was exposed to ionizing radiation of 10 Gy dose. After irradiation, the lenses of the pair of glasses were detached from the frame and analyzed by a UV-VIS spectrophotometer (Fig. 4).

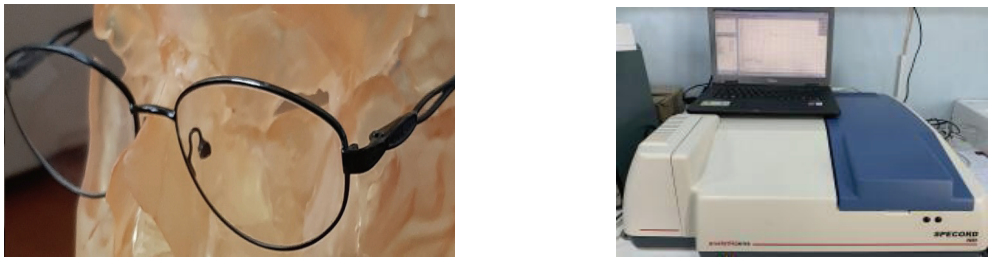

(a) (b)

Fig. 4 – a) 3D phantom of the human head with attached dosimetric glasses;
b) UV-VIS spectrophotometer.

2.2. MONTE CARLO SIMULATION

The MCNP6.2 code was applied for the Monte Carlo simulation. The entire experimental setup including the Co-60 source and its capsule, the lead collimator, dosimeters, head phantom, eyeballs, and eye lenses was modeled by MCNP6.2. A simplified cylindrical phantom based on the results of a previous study [24] was used for phantom simulation. Figure 5 shows the modeled source and the lead conical-shaped collimator. Both sets 1 and 2 of the experiments have been simulated with the exact same conditions. In addition, the uniformity test for two lenses (10 Gy dose) has been simulated as well. The results are presented and discussed in the next section.

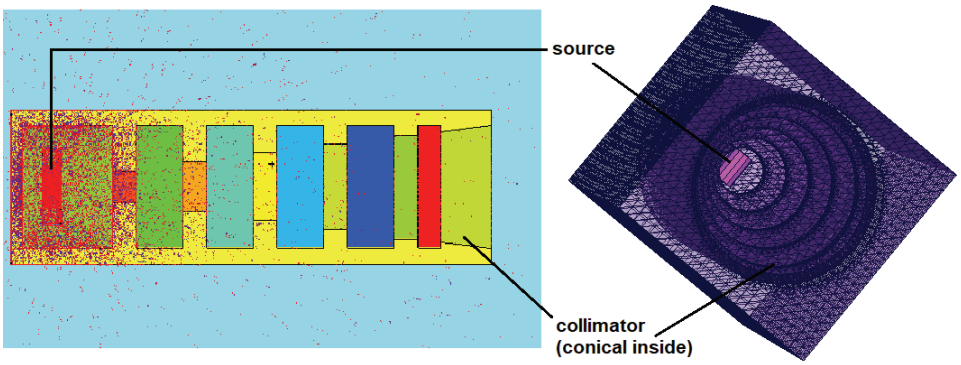

Fig. 5 – Monte Carlo simulation by MCNP6.2. Right: 3D view of the collimator and the source, left: 2D view of the same structure, the particle tracks are also shown in the 2D view.

3. RESULTS AND DISCUSSION

The dose debit in the air (flow rate) of the radioactive Co-60 source, determined by MC simulation (MCNP6.2) and the one obtained experimentally (traceable to the standards of PTB, Germany) are compared in Table 1. It is observed that these two quantities are comparable in terms of the uncertainties of determination (3.02% deviation) so that the reportable (conventional true) value could be considered as their arithmetic mean.

Table 1

Comparison between the dose debit in the air (flow rate) of the radioactive Co-60 source, obtained by experiment and MC simulation

Source-detector distance (cm)	Dose debit simulated by MC (μSv/h)	Experimental dose debit (μSv/h)	Deviation (%)	Conventional true value (μSv/h)
150	107.547	104.300	3.02	105.924

The results (the absorbed dose value by dosimeters) of set 1 of the experiments obtained experimentally and by MC simulation are compared to each other and also compared with the reference doses (PTB traceable values: 200, 400, and 600 μSv) in Table 2. Again, set 1 relates to the normal angel of incident towards the phantom's forehead.

Table 2

Absorbed dose values recorded by OSL detectors (experiments), the results obtained by MC simulations, and the reference values. The conventional true value is the arithmetic mean of the simulation and the experimental results (incident beam towards the forehead)

	Exposure duration (s)	Reference equivalent dose (mSv)	Simulated absorbed dose (mSv)	Experimental absorbed dose (mSv)	Deviation between simulation and experiment (%)	Deviation between simulation and reference (%)	Deviation between experiment and reference (%)	Conventional true value (mSv)
Forehead	6.903×10^3	0.200	0.178	0.190	6.15	10.85	5.00	0.184
	1.381×10^4	0.400	0.357	0.437	18.39	10.85	–9.25	0.397
	2.071×10^4	0.600	0.535	0.647	17.32	10.85	–7.83	0.591
Right eye	6.903×10^3	0.200	0.169	0.192	12.03	15.55	4.00	0.180
	2.071×10^4	0.600	0.507	0.602	15.83	15.55	–0.33	0.554
Left eye	6.903×10^3	0.200	0.164	0.209	21.44	17.90	–4.50	0.187
	2.071×10^4	0.600	0.493	0.598	17.63	17.90	0.33	0.545
Right temple	6.903×10^3	0.200	0.182	0.207	12.27	9.20	–3.50	0.194
	1.381×10^4	0.400	0.363	0.437	16.89	9.20	–9.25	0.400
	2.071×10^4	0.600	0.545	0.620	12.13	9.20	–3.33	0.582
Left temple	6.903×10^3	0.200	0.177	0.207	14.64	11.65	–3.50	0.192
	1.381×10^4	0.400	0.353	0.400	11.65	11.65	0.00	0.377
	2.071×10^4	0.600	0.530	0.637	16.78	11.65	–6.17	0.584

The results of set 2 of the experiments (incident directed towards the right temple) are presented in Table 3 for an equivalent reference dose of 400 μSv (traceable to the PTB standard). Given that the experimental and simulated absorbed dose values presented in both Tables 2 and 3 are comparable in terms of the uncertainties of determination, the reportable (conventional true) value could be considered as their arithmetic mean (last columns in Tables 2 and 3).

Table 3

Absorbed dose values recorded by OSL detectors (experiments), the results obtained by MC simulations, and the reference values. The conventional true value is the arithmetic mean of the simulation and the experimental results (incident beam towards the right temple)

	Exposure duration (s)	Reference equivalent dose (mSv)	Simulated absorbed dose (mSv)	Experimental absorbed dose (mSv)	Deviation between simulation and experiment (%)	Deviation between simulation and reference (%)	Deviation between experiment and reference (%)	Conventional true value (mSv)
Forehead	1.381×10^4	0.400	0.383	0.433	11.58	4.29	–8.25	0.408
Right eye			0.390	0.457	14.74	2.59	–14.25	0.423
Left eye			0.347	0.358	3.02	13.20	10.50	0.353
Right temple			0.396	0.445	11.10	1.09	–11.25	0.420
Left temple			0.329	0.307	–7.15	17.76	23.25	0.318

The spectrophotometer used to determine the uniformity of the ionizing radiation field by the RIA method is Specord 210, Analytik Jena GmbH, Germany (Fig. 4(b)). Following the analysis by the spectrophotometric method, the difference in darkening between the two glass lenses was negligible (much smaller than the uncertainty of the determination method). The spectra of the two lenses are illustrated in Fig. 6. It is evident from Fig. 6 that the darkening density of the two lenses is evenly distributed. Therefore, the ionizing radiation field provided by the radioactive source is homogeneously distributed.

Table 4 shows the results obtained by the Monte Carlo technique to determine the uniformity of the radiation field from exposure to a radioactive source to 10 Gy dose, with the radiation beam towards the forehead. The deviation between the two values obtained (right lens *vs.* left lens) is 2.49%, lower than that given by the determination method. Comparing the results obtained by the two methods of determination (experimental *vs.* computational methods) reveals a high degree of equivalence, confirming the homogeneity of the distribution of the gamma radiation field used at all dosimetric phantom exposures.

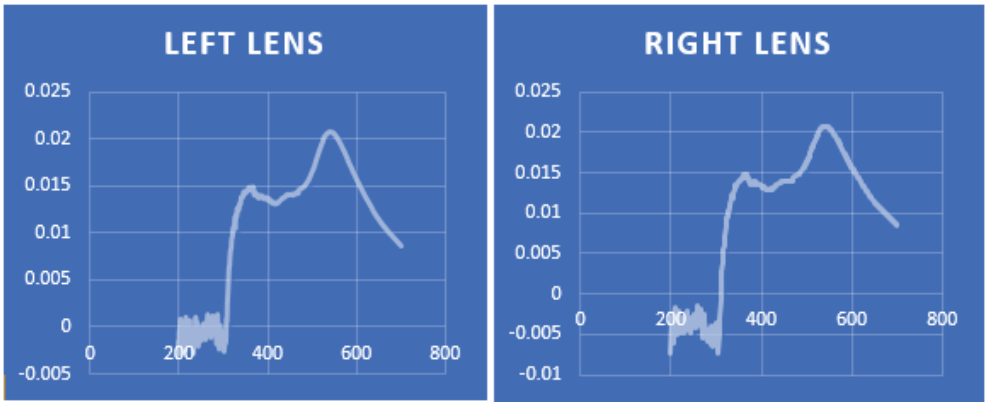

Fig. 6 – UV-VIS Spectra of the eyeglass lenses after exposure to 10 Gy dose.

Table 4

Monte Carlo simulation (MCNP6.2) of the field uniformity determination by exposure the two eyeglass lenses to 10 Gy dose

	Source – phantom's forehead distance (cm)	MC simulated dose (Sv)	The deviation between right and left eyeglass lenses (%)
Right eyeglass lens	150	9.445	2.49
Left eyeglass lens		9.210	

As mentioned before, the final and main step of this work is to provide traceable, reliable, and precise calibration factors with the associated uncertainties for the commercially available dosimeters. To this end, the conventional true values (the arithmetic means between simulations and experiments) of the absorbed dose by the eye lenses have been considered as the national standards. Since in a real situation of eye-lens dosimetry, the commercial dosimeter would be attached to one of the temples (and not directly on the eye), one can obtain a calibration factor for the commercial dosimeter on the temple, using the real spot of exposure (eye lens). Therefore, by multiplying the calibration (multiplicative) factor to the registered dose by the temple's dosimeter, the standard dose value has to be obtained. Here, the dosimeter mounted on the left temple is considered as the commercial one that needs to be calibrated. The conventional true values of the two eyes are considered as the standard doses, for reference doses of 200 and 600 μSv as the extremums and the radiation directed towards the forehead. The results are presented in Table 5.

Table 5

Calibration (multiplicative) factors and uncertainties

	Reference equivalent dose (mSv)	Absorbed dose by the left temple (mSv)	Conventional true value for dose of eyes (mSv)	Calibration (multiplicative) factor	Average value of calibration factor	Uncertainty (%)
Dosimeter on left temple to be calibrated* with respect to right eye	0.200	0.207	0.180	0.869	0.87	0.12
	0.600	0.637	0.554	0.870		
Dosimeter on left temple to be calibrated* with respect to left eye	0.200	0.207	0.187	0.903	0.88	5.21
	0.600	0.637	0.545	0.856		

* The dosimeter mounted on the left temple acts as the commercial dosimeter that needs to be calibrated.

4. CONCLUSION

The main result of this project is a new method for assuring the national metrological traceability chain related to the dosimetry of the eye lens by creating high-precision human head dosimetry phantoms, using state-of-the-art 3D printing techniques. The measurements of the absorbed dose by the eye lenses have been done with a 3D printed head phantom and a standard Co-60 radioactive source. The calibration factors for the dosimeters mounted on the temple (not directly on the eyes) have been obtained with the associated uncertainties, using the OSL dosimeters mounted on the eye lenses. The experimental results have been supported by the Monte Carlo simulation technique and their arithmetic mean (experimental and calculational values) have been considered as the conventional true value.

In this way, the practical implementation of the provisions of the Council Directive 2013/59/EURATOM, as well as the International Standardization Organization (ISO) are strongly supported. Moreover, the relevant national and international organizations and decision-makers could benefit from the scientific/technical output of this work.

Acknowledgements. This work was supported by a grant of the Romanian Ministry of Education and Research, CNCS – UEFISCDI, project number PN-III-P1_1.1-TE-2019-0217, within PNCDI III.

REFERENCES

1. Guidelines for Radiation Protection and Dosimetry of the Eye Lens, *Nederlandse Commissie voor Stralingsdosimetrie* (NCS), Report 31 of the Netherlands Commission on Radiation Dosimetry, 2018.
2. K. Matsubara *et al.*, *Eye lens dosimetry and the study on radiation cataract in interventional cardiologists*, Phys. Med. **44**, 232 (2017).
3. K. Matsubara *et al.*, *A multicenter study of radiation doses to the eye lenses of medical staff performing non-vascular imaging and interventional radiology procedures in Japan*, Phys. Med. **74**, 83 (2020).
4. R. Behrens, J. Engelhardt, M. Figel, O. Hupe, M. Jordan, and R. Seifert, *$H_p(0.07)$ photon dosemeters for eye lens dosimetry: calibration on a rod vs. a slab phantom*, Radiat. Prot. Dosimetry **148(2)**, 139 (2012).
5. Radiological protection – Procedures for monitoring the dose to the lens of the eye, the skin and the extremities, ISO 15382:2015 (www.iso.org/standard/61582.html).
6. T. J. Boal and M. Pinak, *Dose limits to the lens of the eye: International Basic Safety Standards and related guidance*, Annals of the ICRP **44**, 112 (2015).
7. *Implications for occupational radiation protection of the new dose limit for the lens of the eye*, IAEA TECDOC Series No. 1731 (2013).
8. F. Vanhavere *et al.*, *Measurements of eye lens doses in interventional radiology and cardiology: Final results of the ORAMED project*, Radiat. Meas. **46**, 1243 (2011).
9. L. Donadille *et al.*, *Staff eye lens and extremity exposure in interventional cardiology: Results of the ORAMED project*, Radiat. Meas. **46**, 1203 (2011).
10. J. Domienik *et al.*, *Extremity and eye lens doses in interventional radiology and cardiology procedures: first results of the ORAMED project*, Radiat. Prot. Dosim. **144**, 442 (2011).
11. F. Vanhavere *et al. ORAMED: optimisation of radiation protection for medical staff*, 7TH EURADOS Report 2012-02 (2012).
12. A. Elter, S. Dorsch, P. Mann, A. Runz, W. Johnen, and C. P. Karger, *Compatibility of 3D printing materials and printing techniques with PAGAT gel dosimetry*, Phys. Med. Biol. **64**, 04NT02 (2019).
13. T. Kamomae *et al.*, *Three-dimensional printer-generated patient-specific phantom for artificial in vivo dosimetry in radiotherapy quality assurance*, Phys. Med. **44**, 205 (2017).
14. M. Alssabbagh, A. A. Tajuddin, M. Abdulmanap, and R. Zainon, *Evaluation of 3D printing materials for fabrication of a novel multi-functional 3D thyroid phantom for medical dosimetry and image quality*, Rad. Phys. Chem. **135**, 106 (2017).
15. R. Ricotti *et al.*, *Dosimetric characterization of 3D printed bolus at different infill percentage for external photon beam radiotherapy*, Phys. Med. **39**, 25 (2017).
16. D. Adliene, E. Jaselskė, B. G. Urbonavičius, J. Laurikaitienė, V. Rudžianskas, and T. Didvalis, *Development of 3D Printed Phantom for Dose Verification in Radiotherapy for the Patient with Metal Artefacts Inside*, Springer Singapore **68(3)**, 643 (2018).
17. J. Tran-Gia, S. Schlögl, and M. Lassmann, *Design and Fabrication of Kidney Phantoms for Internal Radiation Dosimetry Using 3D Printing Technology*, J. Nucl. Med. **57**, 1998 (2016).
18. R. M. Sanchez, E. Vano, J. M. Fernandez, M. Ginjaume, and M. A. Duch, *Measurements of eye lens doses in interventional cardiology using OSL and electronic dosemeters*, Radiat. Prot. Dosimetry **162(4)**, 569 (2014).
19. E. G. Yukihara and S. W. S. Mckeever, *Optically stimulated luminescence (OSL) dosimetry in medicine*, Phys. Med. Biol. **53**, 79 (2008).
20. A General Monte Carlo N-Particle (MCNP) Transport Code (https://mcnp.lanl.gov).
21. C. J. Werner, J. S. Bull, C. J. Solomon, F. B. Brown, G. W. McKinney *et al.*, *MCNP6.2 Release Notes*, Los Alamos National Laboratory, report LA-UR-18-20808 (2018).
22. C. J. Werner (Ed.) *MCNP user's manual – code version 6.2*, Los Alamos National Laboratory, report LA-UR-17-29981 (2017).
23. https://formlabs.com
24. G. Gualdrini *et al.*, *A new cylindrical phantom for eye lens dosimetry development*, Radiat. Meas. **46**, 1231 (2011).